NON-LINEAR GLOBAL SIZING OF HIGH SPEED PM SYNCHRONOUS GENERATOR FOR RENEWABLE ENERGY APPLICATIONS

Adel El Shahat[1,*], Ali Keyhani[1] & Hamed El Shewy[2]

[1] Mechatronics-Green Energy Lab., Electrical & Computer Engineering Dept., Ohio State University, USA
[2] Department of Electrical Power and Machines Engineering, Zagazig University, Egypt
[*] E-mail: adel.elshahat@ieee.org , ahmed.210@osu.edu, adel2029@yahoo.com

ABSTRACT

This paper presents a step by step sizing procedure of High Speed Permanent Magnet Synchronous Generators (HSPMSGs) for renewable energy applications to be driven by micro-turbines. The final design offers significant reductions in both weight and volume in a power range of 5:500 kW. A rotor length to diameter ratio is used as an important design parameter. The results are depicted by 3D plot figures for a number of machines sizing. The simulation of generators sizing is performed using MATLAB. Then, the paper proposes genetic optimized sizing of High Speed Permanent Magnet Synchronous Generators. These designs have more significant improvement in weights and volumes than usual or classical. Efficiency Maximizer Genetic Sizing is proposed. Finally, Optimum Torque per Ampere Genetic Sizing is predicted. The optimization variables are the same in every optimization process. The genetic results are well depicted by some variables 3D figures for initial and detailed sizing. The simulation of generators sizing is performed using MATLAB, and Genetic Algorithm.

Keywords: *Genetic, High-speed, Optimization, generators, Size, Permanent Magnet, Synchronous*

1. INTRODUCTION

High speed PM generators provide a substantial reduction in size and weight, also higher in power density; because as a machine's speed increases, its size decreases for a given output power. The size, weight, and cost are from the major factors for successful design. The increase of the rotating speed of electrical machines is a way to improve their power / mass ratio and thus the dimensions and weight are reduced and the total efficiency is increased [1]-[5]. For high-speed applications, the rotor aspect ratio, defined as length-to-diameter, is a critical parameter. Stator core losses may be minimized by using laminated steel in stator construction and by not generating frequencies that are too high. The main applications of PMSG are for power generation as part of renewable energy resources and main generators for aircraft, etc. [2] – [9]. The sizing of HSPMSG design must address system topology for good power/volume, low cost, and superior efficiency [1] – [14]. Optimum design of high speed PM alternator is proposed to be used in distributed power generation system with experimental tests are conducted to verify the FEM predictions [8], [9]. The high speed permanent magnet (PM) machine has been widely used in distributed power generation. The high speed generator distributed generation system in comparison with PM Doubly Fed Reluctance Generator for the same application has better electromagnetic property and the PM doubly fed reluctance machine has better mechanical behaviour [31]. Seven configurations of both radial-flux and axial-flux machines give comparisons among PM wind generators of different topologies from 1 kW to 200 kW. Optimization of design data are done and verified by finite element analysis and commercial generator test results [32]. Aspects of PM motor technology and design of brushless PM machines are introduced in [12] and [13]; to be used in this paper.

2. BASIC SELECTIONS

NdFeB is preferred because it is cheaper and more readily available. Therefore, NdFeB magnets are selected for use in PMG, with some conservatively assumed values [13], [14], [15]. TM19, 29 gauge electrical silicon steel is selected for the PMG stator and rotor because it is economical [13], [16], its thin laminations minimize power losses due to the circulating eddy current, and because it has a saturation flux density of about 1.8 T [13], [14].

3. MACHINE DESIGN PARAMETERS

3.1. Stator Mechanical Design

Slotted stators consist of openings around the stator for the armature windings, as shown in Figure 1 (a) are selected.

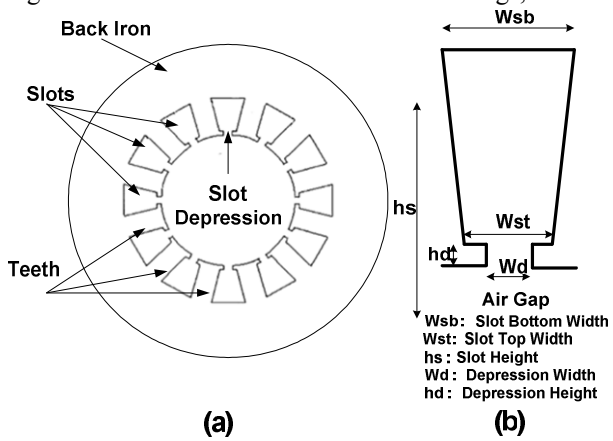

Figure 1. Slotted Stator Design (a) and Stator Slot Geometry (b)

Slots are trapezoidal, but assumed here to be rectangular, as shown in Fig. 1 (b). They contain form-wound windings so that the depression width is the same as the top slot width. Slotting is used because of its advantages [14]. The initial design of the generator assumes a three-phase machine with 36 slots [13].

3.2. Rotor Mechanical Design

For high-speed applications, the rotor aspect ratio, defined as length-to-diameter (L/D), is a critical parameter. PM machines offer flexibility in selecting pole sizes, which allows for smaller diameters. A normal L/D ratio for a wound rotor machine is 0.5 – 1.0, and 1 – 3 for a PM machine [17]. The rotor radius and rotational speed also determine the tip speed of the machine, which is the surface velocity of the rotor.

$$v_{tip} = r\omega_m \tag{1}$$

Where ω_m = angular speed (rad/sec); r = rotor radius (m)
The upper limit on tip speed is between 100-250 m/s, depending on the design of the of machines. In this design, a range of tip speed is taken to be (50:250).

3.3. Number of Poles and Magnets Pole Design

An even number of poles is always used, (here pole pairs number = 3). Assuming a constant mechanical rotation speed, electrical frequency is given as.

$$N(2P) = 120\ f \tag{2}$$

Where N = speed (rpm); P = pole pairs; f = electrical frequency (Hz)
Magnet poles skew factor is selected to reduce cogging torque and smooth out variations in air gap reluctance, flux, and voltage waveforms.

$$k_{sn} = \frac{\sin(n\,\theta_s)}{\frac{\theta_s}{2}} \tag{3}$$

where θ_s: Skew angle, rad E; n: Harmonic number

3.4. Magnetic Dimensions

The magnetic dimensions that affect a PM machine are air gap and magnet height. Air gap flux density (B_g) represents in Eq. 4. The radial air gap is made as small as possible to maximize the air gap flux density, minimize the flux leakage, and to produce a lower reluctance value.

$$B_g = \frac{h_m}{h_m + g} B_r \tag{4}$$

where h_m: Magnet height (mm); g: Air gap (mm); B_r: Magnet Remnant Flux Density (T)
Magnets losses are reduced, using smaller magnets. For uniform magnetic fields, the magnet height is usually larger than the air gap, by a factor 5 – 10.

3.5. Slots Per Pole, Per Phase

Three-phase machines are typically used in this study as the standard choice for most motors and generators.
Another important design parameter is the number of slots per pole, per phase (m), as in Eq. 5.

$$m = \frac{N_s}{2 * P * q} \tag{5}$$

3.6. Stator Windings

The pitch of a winding (α) refers to the angular displacement between the sides of a coil. The breadth of a stator winding results from the coils occupying a distribution of slots within a phase belt. In smaller machines, coils are composed of round insulated wires that are placed in the stator slot, along with insulation material. A slot fill factor (λ_s) is used to determine how much of the slot's cross-sectional area is occupied by winding material, as in Eq. 6.

$$\lambda_s = \frac{Winding \quad Area}{Total \quad Slot \quad Area} \tag{6}$$

Typically, machines contain two coils sides per slot, making the winding a double-layer design [13]. Overall, slot fill factors vary in value from 0.3 – 0.7, depending on the number and size of the conductors in the slots, as well as the amount of labor utilized. A slot fill factor of 0.5 is assumed.

3.7. Machine Calculated Parameters

Each phase of the machine is modeled, as shown in Fig. 2.

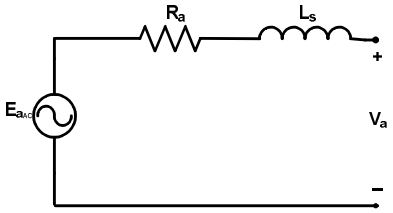

Figure 2. A Per Phase Electrical Model

Where R_a: Armature resistance; L_s: Synchronous inductance; E_a: Back e.m.f voltage and V_a : Terminal voltage.

3.8. Winding Resistances

Copper phase windings resistance is calculated in Eq. 7.

$$R_a = \frac{l}{\sigma * A_{ac}} \tag{7}$$

where l: length of conductor, σ: winding conductivity, A_{ac}: winding cross – sectional area

$$A_{ac} = \frac{A_s * \lambda_s}{2 * N_C} \tag{8}$$

where A_s: slot Area, N_C: turns per coil
But the above stator resistance equation may be used as in low frequencies applications, so it has to be developed. Since the machine rotates at high speed, and high frequency and so the skin depth may be affected. In conductors that carry high frequency currents, skin effect can become an issue and affect the operation of the machine. Skin effect is caused by eddy currents in the windings themselves due to the changing magnetic field. These eddy currents force the current flowing in the conductor to crowd to the outer edges of the conductor. This in turn causes the current to flow through a smaller cross – sectional area and increase the resistance of the conductor. It is well known that, when conductive material is exposed to an ac magnetic field, eddy currents are induced in the material in accordance with Lenz's law. The power loss resulting from eddy currents which can be induced in the slot

conductors appears as an increased resistance in the winding. To understand this phenomenon, let us consider a rectangular conductor as shown in fig. 3. The average eddy current loss in the conductor due to a sinusoidal magnetic field in the y direction is given approximately by Hanselman [12].

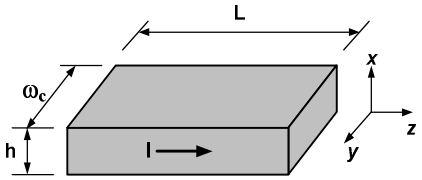

Figure 3. Rectangular conductor geometry

$$P_{ec} = \frac{1}{12}\sigma L\,\omega_c h^3 \omega^2 u_0^2 H_m^2 \tag{9}$$

Where H_m: the turn field intensity value; u_0: perm. of free space.
Since skin depth is defined as

$$\delta = \sqrt{\frac{2}{\omega u_0 \sigma}} \tag{10}$$

Equation (9) can be written as

$$P_{ec} = \frac{L\,\omega_c h^3}{6\sigma\delta^4} H_m^2 \tag{11}$$

Using this expression it is possible to compute the ac resistance of the slot conductors. If the slot conductors are distributed uniformly in the slot, and substituting the field intensity into eq. (11) and summing over all n_s conductors gives a total slot eddy current loss of

$$P_e = (\frac{d_s L h^2 n_s^2}{9\sigma\delta^4 \omega_s}) I^2 \tag{12}$$

Where I: rms conductor current; ω_s: Slot width (m); d_s: Slot depth (m)
The slot resistance of a single slot containing ns conductors connected in series is

$$R_{sl} = \frac{\rho n_s^2 L}{k_{cp}\omega_s d_s} \tag{13}$$

L: the slot length; k_{cp}: the conductor packing factor, is the ratio of cross sectional area occupied by conductors to the entire slot area and ρ: electrical resistivity (Ω.m).
Using eq. (13), the total slot resistance can be written as

$$R_{st} = R_{sl} + R_{ec} = R_{sl}(1 + \Delta_e) \tag{14}$$

In this equation, $\Delta e = R_{ec}/R_{sl}$ is the frequency-dependent term. Using eq. (13) and eq. (12), this term simplifies to

$$\Delta_e \equiv \frac{R_{ec}}{R_{sl}} = \frac{1}{9}(\frac{d_s}{\delta})^2 (\frac{h}{\delta})^2 \tag{15}$$

This result shows that the resistance increases not only as a function of the ratio of the conductor height to the skin depth but also as a function of the slot depth to the skin depth. Thus, to minimize ac losses, it is desirable to minimize the slot depth as well as the conductor dimension. For a fixed slot cross-sectional area, this implies that a wide but shallow slot is best.

3.9. Winding and Magnet Factors

Winding are short-pitched and have breadth associated with them. To account for these effects, a winding factor (k_w) is utilized, as in Eq. 16.

$$k_{wn} = k_{pn} * k_{bn} \tag{16}$$

Short-pitching is an important means for eliminating harmonics and improving the power quality of the machine. The pitch factor is shown in Eq. 17.

$$k_{pn} = \sin(\frac{n*\alpha}{2}) * \sin*\ (\frac{n*\pi}{2}) \tag{17}$$

The breadth factor explains the effect of the windings occupying a distribution or range of slots within a phase belt. The breadth factor is derived in Eq. 18.

$$k_{bn} = \frac{\sin(\frac{n*m*\gamma}{2})}{m*\sin(\frac{n*\gamma}{2})} \quad (18)$$

Where m: slots per pole per phase; γ: coil electrical angle

The magnetic flux factor equation [12], for the slotted stator and surface magnet configuration is shown in Eq. 19.

$$k_{gn} = \frac{R_i^{np-1}}{R_s^{2np} - R_i^{2np}} * [(\frac{np}{np+1}) * (R_2^{np+1} - R_1^{np+1}) + \frac{np}{np-1} * R_s^{2np} * (R_1^{1-np} - R_{v2}^{1-np})] \quad (19)$$

Where R_s: outer magnetic boundary, R_2: outer boundary of magnet; R_i: inner magnetic boundary, R_1: inner boundary of magnet

3.10. Flux, and Voltage

For useful voltage, only the fundamental components are used to determine the internal voltage (back e.m.f) of the generator, as shown in Equations 20, 21, and 22.

$$E_a = \omega_0 \lambda \quad (20)$$

$$\lambda = \frac{2*R_s*L_{st}*N_a*k_w*k_s*B_1}{P} \quad (21)$$

$$B_1 = \frac{4}{\pi} * B_g * k_g * \sin(\frac{P\theta_m}{2}) \quad (22)$$

where θ_m: magnet physical angle

$$B_g = \frac{k_l C_\phi}{1 + k_r * \frac{u_{rec}}{PC}} * B_r \quad (23)$$

where u_{rec}: recoil permeability; B_r: remnant flux density

$$PC = \frac{h_m}{g_e * C_\phi} \quad (24)$$

Where PC: permeance coeff.; C_Φ: flux concentration factor (Am/Ag)

$$N_a = 2 * P * N_c \quad (25)$$

where N_c : Turns per coil; N_a : Number of armature turns (each slot has 2 half coils)

$$\tau_s = w_s + w_t ; g_e = k_c * g \quad (26)$$

Where g_e: effective air gap; w_s: average slot width; w_t: tooth width

Here, a leakage factor ($K_l \sim 0.95$) and a reluctance factor ($K_r \sim 1.05$) are both used for surface magnets. The presence of the slots in the stator also affects the air gap flux density because of the difference in permeance caused by the slots. Carter's coefficient (k_c) is used to account for this effect [12].

$$k_c = [1 - \frac{1}{\frac{\tau_s}{w_s} * (5 * \frac{g}{w_s} + 1)}]^{-1} \quad (27)$$

The terminal voltage (V_a) is calculated from the internal voltage (E_a), and the synchronous reactance voltage drop. The armature resistance is usually ignored because it is much smaller than synchronous reactance. The voltage is found as a relation in output power (P_{wr}), e.m.f, and reactance from the resulting quadratic equation.

$$V_a = \sqrt{\frac{-BB + \sqrt{BB^2 - 4CC}}{2}} \quad (28)$$

Where $BB = \frac{2}{3} X_s P_{wr} - E_a^{\,2};\ CC = \frac{2}{9} X_s^{\,2} P_{wr}^{\,2}$

3.11. Machine Inductances

In a slotted PM machine, there are three distinct components of inductance: the largest, air gap inductance slot leakage inductance, and the smallest, end-turn inductance. The total inductance for the phase is the sum of the three inductances, ignoring other small factors.

$$L_s = L_{ag} + L_{slot} + L_e; \quad X_s = \omega_0 * L \tag{29}$$

The air gap inductance is given by Eq. 30.

$$L_{ag} = \frac{\lambda}{i} = \frac{q}{2} * \frac{4}{n\pi} * \frac{u_0 * R_s * L_{st} * N_a^{\,2} * k_{wn}^{\,2}}{n^2 * P^2 * (g + h_m)} \tag{30}$$

The slot leakage inductance is presented in Equation 31. Assume the slot is rectangular with slot depressions, as in Figure 1, and assume (m) slots per pole per phase, with a standard double layer winding.

$$L_{slot} = L_{as} - L_{am}; (3phase) \tag{31}$$

$$L_{am} = 2 * P * L_{st} * Perm * N_{sp} * N_c^{\,2} \tag{32}$$

$$L_{as} = 2 * P * L_{st} * Perm * [4 * N_c^{\,2} (m - N_{sp}) + 2 * N_{sp} * N_c^{\,2}] \tag{33}$$

A slot permeance per unit length is shown in Equation 34.

$$Perm = \frac{1}{3} * \frac{h_s}{w_{st}} + \frac{h_d}{w_d} \tag{34}$$

The end turn inductance is introduced in Equation 35, assuming the end turns are semi-circular, with a radius equal to one-half the mean coil pitch.

$$L_e = \frac{u_0 * N_c * N_a^{\,2} * \tau_s}{2} * \ln\left(\frac{\tau_s * \pi}{\sqrt{2 * A_s}}\right) \tag{35}$$

3.12. Basic Losses

Losses in a machine consist of core losses, conductor losses, friction and windage losses, and rotor losses. Rotor losses will be discussed later. Stator core losses, per weight, can be greater than normal in machines because of higher frequencies. These losses are minimized by using laminated steel in stator construction and by not generating frequencies that are too high. Core losses consist of hysteresis and eddy current losses. The best way to approximate core losses is to use empirical loss data. An exponential curve fitting is applied to the empirical data for M-19, 29 gauge material, in order to obtain an equation for estimating core losses, as in Equation 36, with constant values in [19].

$$P_C = P_0 * \left(\frac{B}{B_0}\right)^{\varepsilon B} * \left(\frac{f}{f_0}\right)^{\varepsilon f} \tag{36}$$

where P_0: Base power; B_0: Base flux density; ε_B: Flux density exponent; f_0: Base frequency; ε_f: Frequency exponent
The above commonly used equation considering hysteresis and eddy-current loss is not completely satisfactory, because the measured iron loss is much higher than theoretically calculated. This is so because it assumes a homogenous magnetization of the laminations, which is not a valid representation of what happens during the magnetization process. The loss caused by the movements of the magnetic domain walls is higher than the loss calculated with the commonly used equation. The difference between measured and calculated loss is called the excess loss or the anomalous loss. Sometimes, this anomalous or excess loss is considered as a third contribution to the iron loss. Great efforts have been made to calculate this excess loss, because of the complexity of the domain patterns. For reasons mentioned before, it is useful to represent the core loss by core loss resistance, which is placed in equivalent circuit. The core loss resistance is connected across the voltage V_a. Therefore, the power dissipated in this resistance is [22-30].

$$P_{R_c}(\omega) = \frac{V_a^2}{R_c} \tag{37}$$

$$R_c(\omega) = \frac{3\pi^2 {L_{st}}^2 N_a^2 \sqrt{\omega}}{8 c_{Fe} k_{Fe} (\frac{1}{\omega_0})^{1.5} (\frac{1}{B_0})^2 \{m_{st} (\frac{p\beta_{slot}}{b_{st}})^2 + m_{sy} (\frac{1}{h_{sy}})^2\}} \tag{38}$$

Where R_c: core resistance, c_{Fe}: correction factor for iron loss calculation, b_{st}: stator tooth width, k_{Fe}: specific iron loss, m_{st}: stator teeth mass, βslot: slot angle, h_{sy}: stator yoke height

When this core loss resistance is depicted in an equivalent circuit, it should be noted that the resistance is frequency dependent. The conductor losses are found, using Eq. 39.

$$P_a = q * I_a^2 * R_a \tag{39}$$

For rotors operating at high speed, the friction and windage in air can cause losses which result in inefficiency and heat production. These losses are calculated, using the power necessary to overcome the drag resistance of a rotating cylinder, as given by Eq. 40 [20].

$$P_{wind} = C_f * \pi * \rho_{air} * \omega^3 * R^4 * L_{st} \tag{40}$$

The coefficient of friction can be approximated by Eq. 41.

$$C_f \cong 0.0725 * \mathrm{Re}y^{-0.20} \tag{41}$$

where Rey: Reynold's Number

4. SIZING METHOD

For the basic sizing calculations, an air-cooled generator is assumed with 10 psi [13], [21]. The machine power equation is utilized to derive the rotor radius and stack length of the machine, as in Equation 42.

$$P_{wr} = 2 * \pi * r * L_{st} * v_{tip} * \tau \tag{42}$$

where r = rotor radius; L_{st} = stack length; τ = shear stress (psi)

The L/D ratio is substituted for L_{st}. Using shear stress, rotor tip speed, and machine power rating range, the power equation is calculated to obtain rotor radius and stack length, while matching the desired rotational speed of the machine with a L/D ratio. Using a pole pair value of 3, a slot height of 10 mm, and a slot fill fraction of 0.5, the frequency is found. Once the basic sizing of the machine is complete, in-depth analysis is conducted to obtain the overall performance within the power range of 5: 500 KW generators. Using the equations presented in previous sections, all the detailed parameters can be obtained. The lengths, volumes, masses, and overall generator parameters are calculated, using basic geometric equations and relationships. A 15% service mass fraction is added to the total mass estimate to account for the additional services associated with machines cooling [14], [21]. Once the mass of each of the stator parts is known, core losses are estimated. The calculation of lengths, volumes, and weights are presented. The mass of armature conductors, core mass, magnet mass, and shaft mass are calculated to give the total mass value. Finally, stator resistance, terminal voltage, current, loss types, input power, and efficiency are calculated.

$$M_{Total} = M_{Core} + M_{Magnet} + M_{Shaft} + M_{Conductor} + M_{Service} \tag{43}$$

$$M_{core} = M_{cb} + M_{ct} \tag{44}$$

$$M_{cb} = \rho_s \pi (R_{co}^2 - R_{ci}^2) L_{st} \tag{45}$$

Where M_{cb}: back iron mass (kg); : steel density (kg/m^3); R_{co}: core outside radius; R_{ci}: core inside radius

$$R_{ci} = R + h_m + g + h_d + h_s \tag{46}$$

where hm: Magnet thickness(m); g: air gap (m); hd: slot depression depth(m); hs: slot depth (m)

$$R_{co} = R_{ci} + dc \tag{47}$$

where dc: stator core back iron depth (m)

$$M_{ct} = \rho_s L_{st} (N_s w_t h_s + 2 \pi R h_d - N_s h_d w_d) \tag{48}$$

where M_{ct}: teeth mass; N_s: number of slots; w_t: tooth width; w_d: slot depression width(m)

$$M_{Magnet} = 0.5 (p \theta_m ((R + h_m)^2 - R^2) L_{st} \rho_m \tag{49}$$

where θ_m: Magnet physical angle(rad); ρ_m: Magnet density; p: pole pairs number

$$M_{Shaft} = \pi R^2 L_{st} \rho_s \tag{50}$$

$$M_{Conductor} = 3 L_{ac} A_{ac} \rho_c \tag{51}$$

where L_{ac}: armature conductor length; A_{ac}: armature conductor area (assumes form wound); ρ_c: conductor density

$$L_{ac} = 2 N_a (L_{st} + 2 l_{e2}) \tag{52}$$

$$A_{ac} = A_s \lambda_s / (2 N_c) \tag{53}$$

where N_a: number of armature turns; l_{e2}: end length (half coil); A_s: slot area; λ_s: slot fill fraction; N_c: turns per coil

A 15% service mass fraction is added to the total mass estimate to account for the additional services associated with machines cooling [21].

$$M_{Service} = 0.15 (M_{Conductor} + M_{Shaft} + M_{Magnet} + M_{Conductor}) \tag{54}$$

The efficiency

$$\eta = P_{out} / P_{input} \tag{55}$$

$$P_{input} = P_{Total\_Losses} + P_{out} \tag{56}$$

5. CLASSICAL SIZING RESULTS

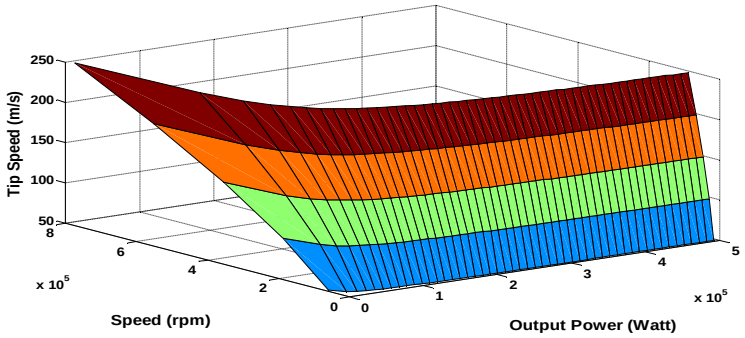

Figure 4. Output Power with Speed Relations at Various Tip Speeds

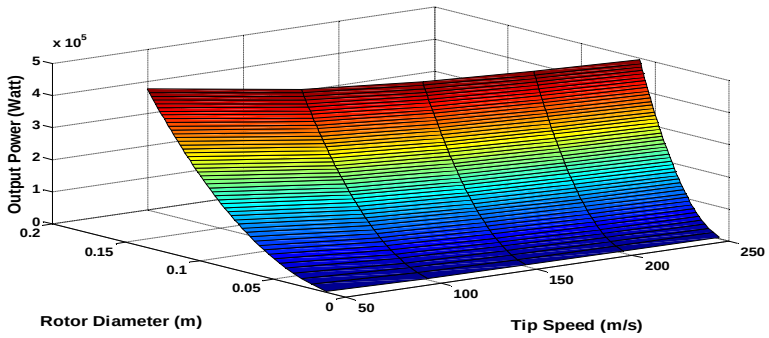

Figure 5. Output Power with Rotor Diameter Relations at Various Tip Speeds

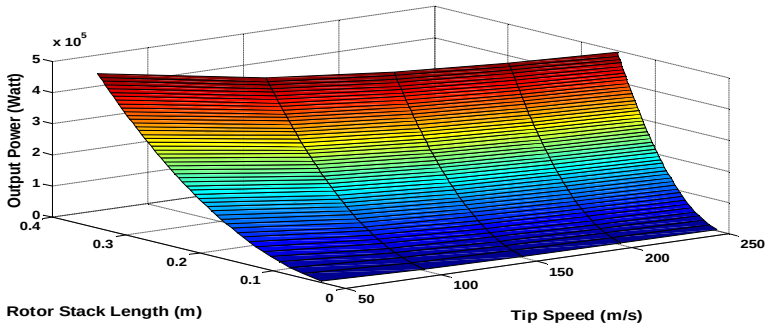

Figure 6. Power with Rotor Stack Length Relations at Various Speeds

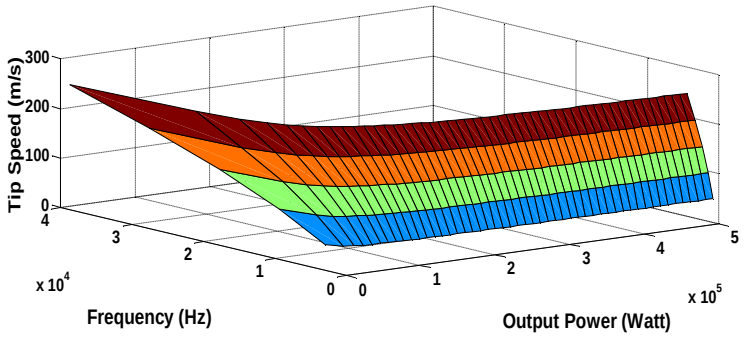

Figure 7. Output Power with Frequency Relations at Various Tip Speeds

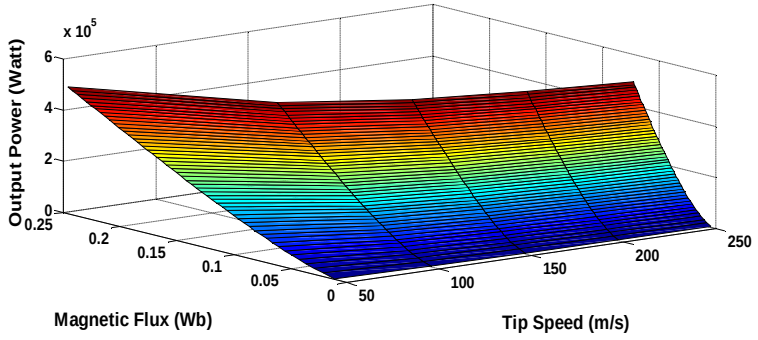

Figure 8. Power with Magnetic Flux (Wb) Relations at Various Tip Speeds

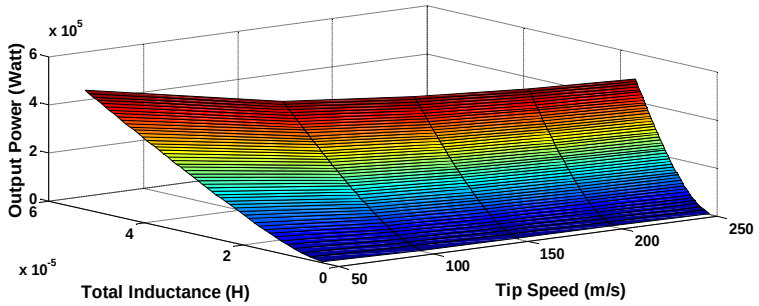

Figure 9. Power with Total Inductance (H) Relations at Various Tip Speeds

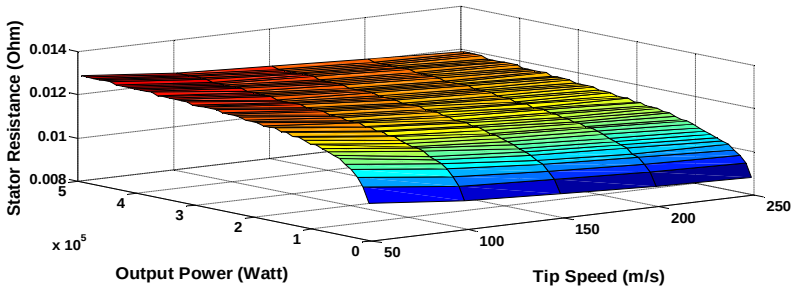

Figure 10. Output Power with Stator Resistance Relations at Various Tip Speeds

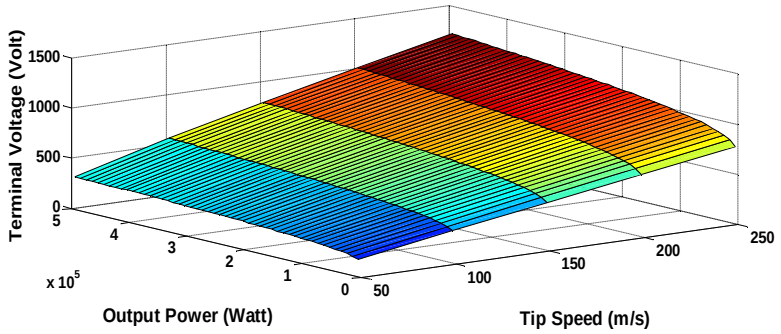

Figure 11. Power with Terminal Voltage Relations at Various Tip Speeds

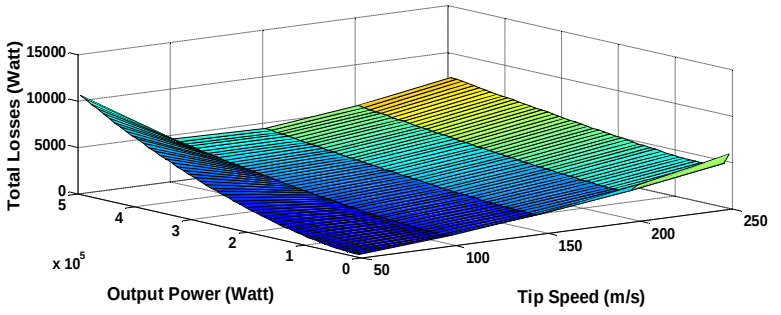

Figure 12. Output Power with Total Loss Relations at Various Tip Speeds

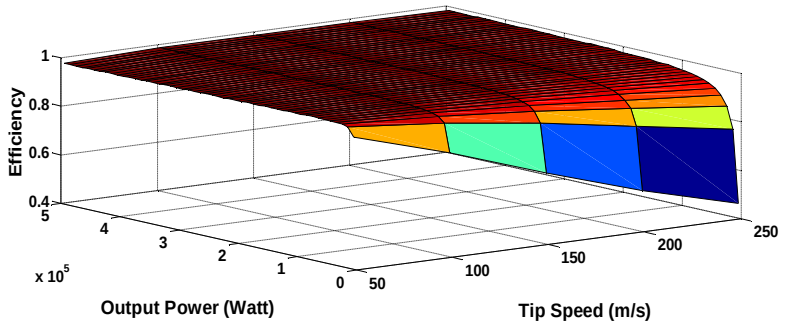

Figure 13. Output Power with Efficiency Relations at Various Tip Speeds

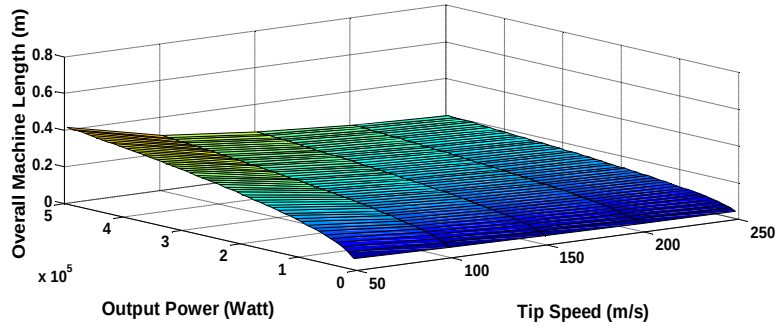

Figure 14. Power with Overall Machine Length Relations at Tip Speeds

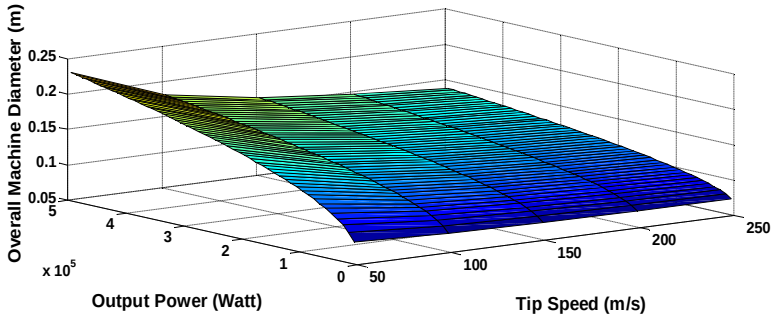

Figure 15. Output Power with Overall Diameter Relations at Various Tip Speeds

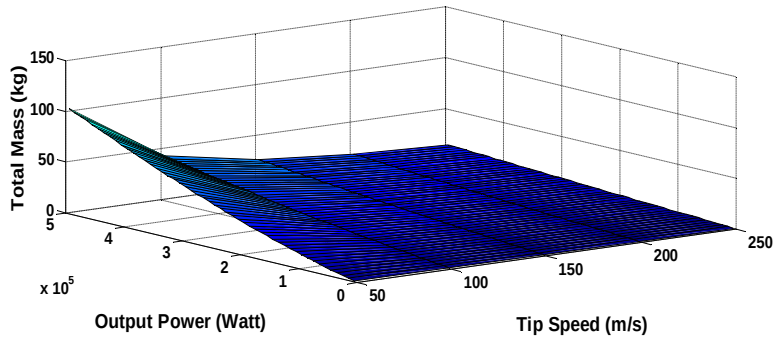

Figure 16. Output Power with Total Mass Relations at Various Tip Speeds

6. GENETIC ALGORITHM HSPMSG SIZING

The genetic algorithm is a method for solving both constrained and unconstrained optimization problems that is based on natural selection, the process that drives biological evolution. The genetic algorithm repeatedly modifies a population of individual solutions. At each step, the genetic algorithm selects individuals at random from the current population to be parents and uses them to produce the children for the next generation. Over successive generations, the population "evolves" toward an optimal solution. We can apply the genetic algorithm to solve a variety of optimization problems that are not well suited for standard optimization algorithms, including problems in which the objective function is discontinuous, non - differentiable, stochastic, or highly nonlinear.
The genetic algorithm uses three main types of rules at each step to create the next generation from the current population:
• Selection rules select the individuals, called parents, which contribute to the population at the next generation.
• Crossover rules combine two parents to form children for the next generation.
• Mutation rules apply random changes to individual parents to form children.
The genetic algorithm differs from a classical, derivative-based, optimization algorithm in two main ways, as summarized in the following:
Classical Algorithm: generates a single point at each iteration, in which the sequence of points approaches an optimal solution, also it selects the next point in the sequence by a deterministic computation.
Genetic Algorithm: generates a population of points at each iteration, in which the best point in the population approaches an optimal solution, moreover it selects the next population by computation which uses random number generators.

6.1. How the Genetic Algorithm Works?

The following outline summarizes how GA works:
1. Algorithm begins by creating a random initial population.
2. The algorithm then creates a sequence of new populations. At each step, the algorithm uses the individuals in the current generation to create the next population. To create the new population, the algorithm performs the following steps:
   a. Scores each member of the current population by computing its fitness value.
   b. Scales the raw fitness scores to convert them into a more usable range of values.
   c. Selects members, called parents, based on their fitness.
   d. Some of the individuals in the current population that have lower fitness are chosen as elite. These elite individuals are passed to the next population.
   e. Produces children from the parents. Children are produced either by making random changes to a single parent mutation or by combining the vector entries of a pair of parents crossover.
   f. Replaces the current population with the children to form the next generation.
3. GA stops when one of the stopping criteria is met.

6.2. Description of the Nonlinear Constraint Solver

The genetic algorithm uses the Augmented Lagrangian Genetic Algorithm (ALGA) to solve nonlinear constraint problems. The optimization problem solved by the ALGA algorithm is min x f (x), such that

$$\begin{aligned} &ci\,(x) \le 0,\ i = 1 \ldots.. m \\ &ceqi\,(x) = 0,\ i = m+1 \ldots mt \\ &A \,.\, x \le b \\ &Aeq \,.\, x = beq \\ &lb \le x \le ub, \end{aligned} \qquad (57)$$

Where c (x) represents the nonlinear inequality constraints, ceq (x) represents the equality constraints, m is the number of nonlinear inequality constraints, and mt is the total number of nonlinear constraints.
The Augmented Lagrangian Genetic Algorithm (ALGA) attempts to solve a nonlinear optimization problem with nonlinear constraints, linear constraints, and bounds. In this approach, bounds and linear constraints are handled separately from nonlinear constraints. A sub problem is formulated by combining the fitness function and nonlinear constraint function using the Lagrangian and the penalty parameters. A sequence of such optimization problems are approximately minimized using the genetic algorithm such that the linear constraints and bounds are satisfied.
A sub - problem formulation is defined as

$$\Theta(x,\lambda,s,\rho) = f(x) - \sum_{i=1}^{m}\lambda_i s_i \log(s_i - c_i(x)) + \sum_{i=m+1}^{mt}\lambda_i c_i(x) + \frac{\rho}{2}\sum_{i=m+1}^{mt} c_i(x)^2 \quad (58)$$

where the components λi of the vector (λ) are nonnegative and are known as Lagrange multiplier estimates. The elements si of the vector (s) are non – negative shifts, and ρ is the positive penalty parameter. The algorithm begins by using an initial value for the penalty parameter (Initial Penalty).

The genetic algorithm minimizes a sequence of the sub – problem, which is an approximation of the original problem. When the sub - problem is minimized to a required accuracy and satisfies feasibility conditions, the Lagrangian estimates are updated. Otherwise, the penalty parameter is increased by a penalty factor (Penalty Factor). This results in a new sub – problem formulation and minimization problem. These steps are repeated until the stopping criteria are met. For a complete description of the algorithm, see the references [35], [36].

6.3. Efficiency Maximizer Genetic Sizing

The optimization variables here are: x1, x2, and x3, are L/D ratio, rotor radius, and rotor stack length respectively. Then implement the efficiency function, in the form of m. file. After that, using the Genetic Algorithm, with the previous technique, to maximize the function and generate the desired variables for this maximization or by more accurate word by optimizing this function with a simple constraints that are [1 0 0] as lower limit, and [3 1 1] as upper limit. Using these optimizing variables, we can deliver all detailed variables for the desired HSPMSG at maximum efficiency. The following are some examples from the results of the efficiency maximizing function at tip speeds of 250, 200, and 150 m/s, with a sample output power range from 50: 500 Kw. Also, it is important to adjust all options in the Genetic GUI by in a proper manner, especially mutation function one, also the population, selection, and stopping criteria …… etc.

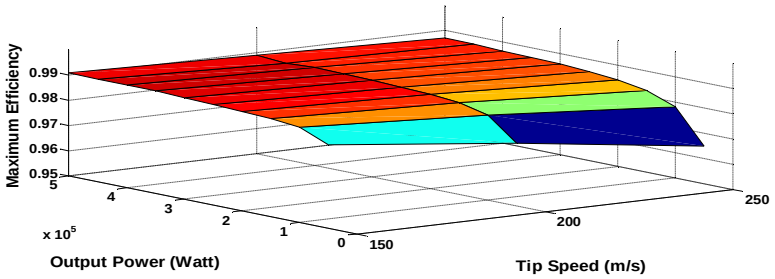

Figure 17. Maximum Efficiency with Tip Speed and Output Power

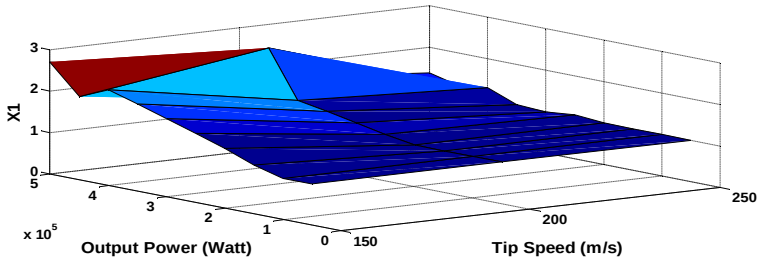

Figure 18. X1 with Tip Speed and Output Power

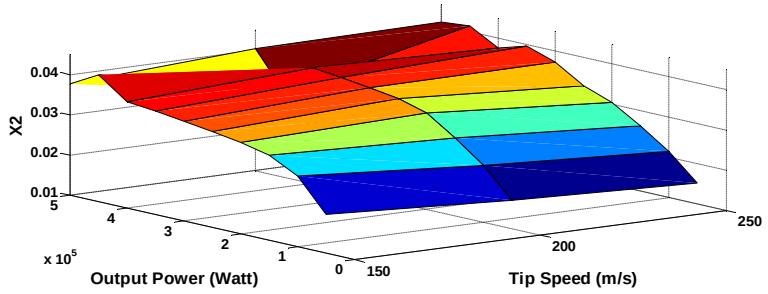

Figure 19. X2 with Tip Speed and Output Power

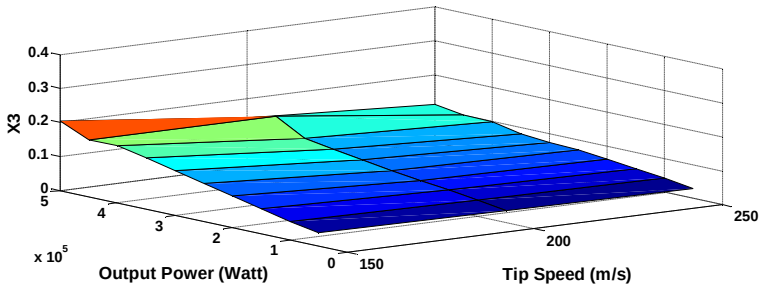

Figure 20. X2 with Tip Speed and Output Power

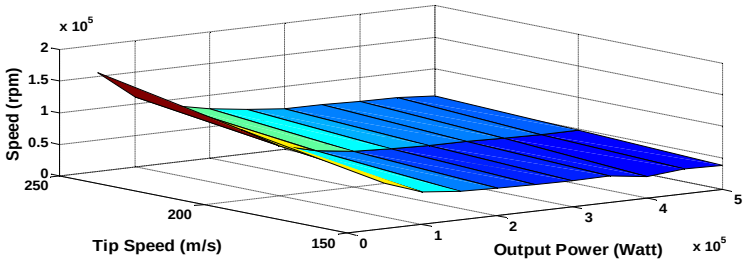

Figure 21. Speed (rpm) with Tip Speed and Output Power

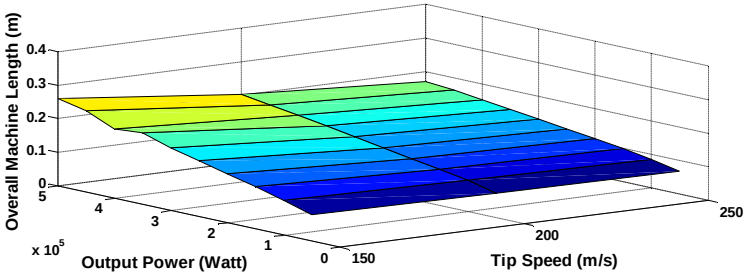

Figure 22. Overall Machine Length with Tip Speed and Output Power

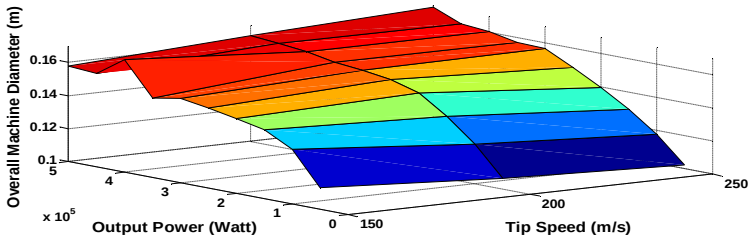

Figure 23. Overall Machine Diameter with Tip Speed and Output Power

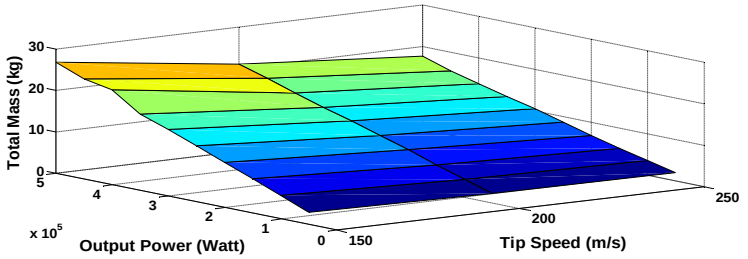

Figure 24. Total Mass with Tip Speed and Output Power

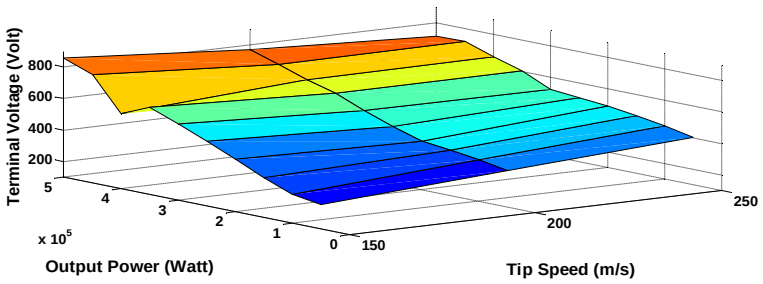

Figure 25. Terminal Voltage with Tip Speed and Output Power

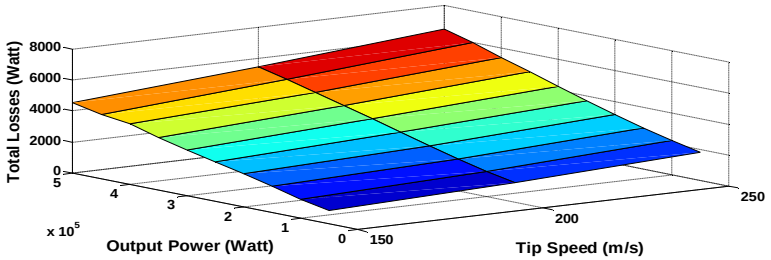

Figure 26. Total Losses with Tip Speed and Output Power

6.4. Optimum Torque per Ampere Genetic Sizing

Optimum torque per ampere control is considered as one of famous PM synchronous machine control strategies. So as a new idea or a question arise, why we can not design optimum torque per ampere HSPMSM with the aid of genetic algorithm? The answer is, here this is a trial to present this idea. The optimization variables here are the same, that x1, x2, and x3, are L/D ratio, rotor radius, and rotor stack length respectively. Then implement the optimum torque per ampere function as fitness function, in the form of m. file. After that, using the Genetic Algorithm, with the previous technique, to maximize the function and generate the desired variables for this maximization or by more accurate word by optimizing this function with a simple constraints that are [1 0 0] as lower limit, and [3 1 1] as upper limit. Using these variables, we can deliver all detailed variables for the desired HSPMG at optimum torque per ampere. The following are some examples from the results of the torque per ampere maximizing function at tip speeds of 250, and 200 m/s, with a sample output power range from 100: 500 Kw with step of 100 kW. Also, the main notice is to set all options in the Genetic GUI by in a proper manner, especially mutation function one, also the population, selection, and stopping criteria …… etc have to be adjusted. As in the design equations before, the power factor is considered as 0.999999 ≈ 1. So as a valid approximation the torque per ampere could be presented as MTA = 3 Ea / ωe, and this expression is used in MATLAB m.file function.

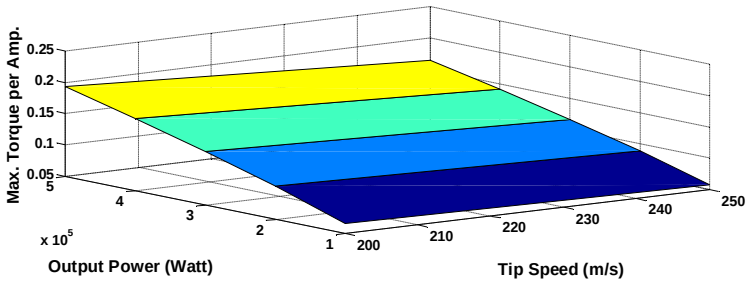

Figure 27. Max. Torque Amp. with Tip Speed and Output Power relations

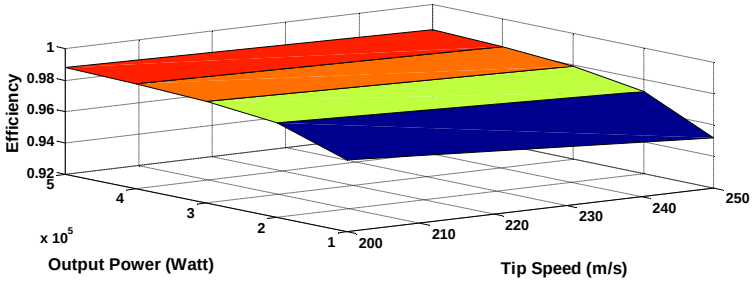

Figure 28. Efficiency with Tip Speed and Output Power relations

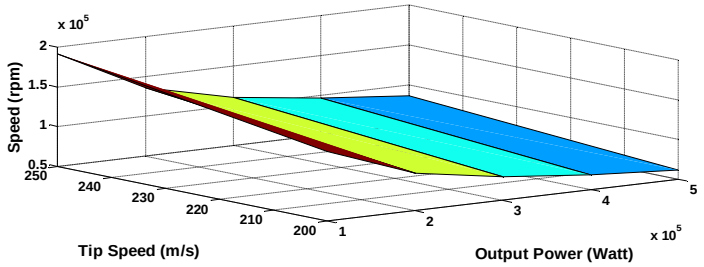

Figure 29. Speed (rpm) with Tip Speed and Output Power relations

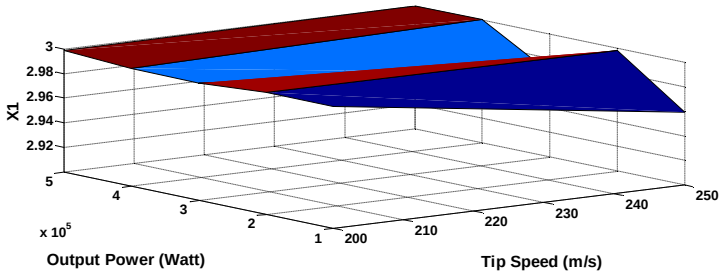

Figure 30. X1 with Tip Speed and Output Power relations

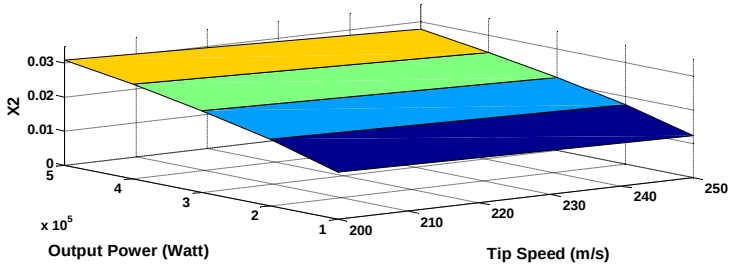

Figure 31. X2 with Tip Speed and Output Power relations

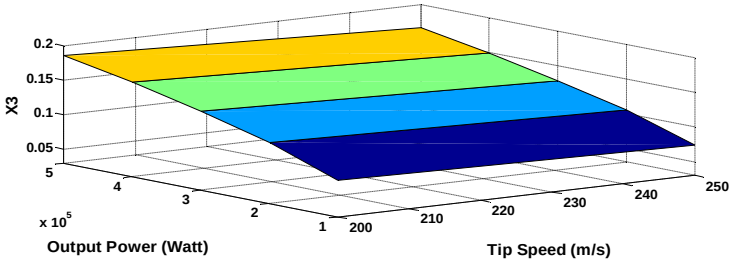

Figure 32. X3 with Tip Speed and Output Power relations

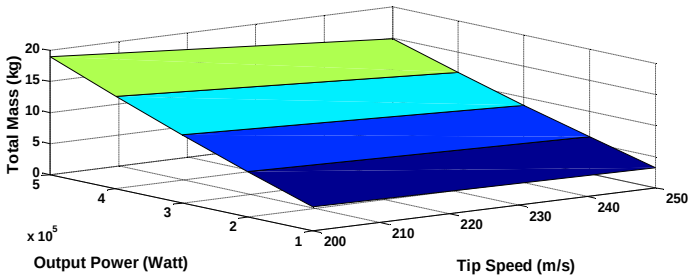

Figure 33. Total Mass with Tip Speed and Output Power relations

It is clear, from this technique, a noticeable improvement appears on the performance parameters. Like this high range of speed, could be obtained, according to its applications.

7. CONCLUSIONS

The sizing method presented gives a step by step method for high speed PM generator design. This paper illustrates the benefits of HSPM generators, compared to the original PM synchronous generators, since it offers significant reductions in both weights and volumes. It discusses the electrical and magnetic sizing of HSPMGs, within the power range of 5:500 Kw and tip speed in the range of 50:250 m/s. The optimizing variables are rotor length to diameter ratio, rotor radius, and stack length, for each of the functions, in the genetic algorithm. It was found that using the genetic algorithm in HSPMSG sizing will solve both constrained and unconstrained optimization problems. The results of the genetic algorithm are presented with the same optimization variables, but the fitness functions, in which the constraints are varied for both efficiency maximization and genetic sizing. We have observed that this will have the benefit of limiting machines losses as in optimum torque per ampere sizing. In our study, we have found that a noticeable improvement appears in the performance parameters.

8. REFERENCES

[1] R. A. Ahmad, Z. Pan, and D. M. Saban, "On-Board Electrical Network Topology Using High Speed Permanent Magnet Generators," Electric Ship Technologies Symposium, 2007. ESTS apos;07. IEEE Volume , Issue , 21-23, pp.356 – 362, May 2007.

[2] S. Scridon, I. Boldea, L. Tutelea, F. Blaabjerg, and E. Ritchie, "BEGA – A Biaxial Excitation Generator for Automobiles: Comprehensive Characterization and Test Results," IAS, 2004, Industry Applications Conference, 2004. 39th IAS Annual Meeting. Conference Record of the 2004 IEEE, vol.3, pp. 1682 – 1690, 3-7 Oct. 2004.

[3] A. Binder, T. Schneider, and M. Klohr, "Fixation of Buried and Surface- Mounted Magnets in High-Speed Permanent-Magnet Synchronous Machines," IEEE Trans. On Industry Applications, Vol. 42, NO. 4, pp. 1031 - 1037, July/August, 2006.

[4] S. M. Hosseini, M. A. Mirsalim, and M. Mirzaei1, "Design, Prototyping, and Analysis of a Low Cost Axial-Flux Coreless Permanent-Magnet Generator," IEEE Trans. On Magnet., Vol. 44, No. 1, pp. 75 – 80, Jan. 2008.

[5] P.H. Mellor, S.G. Burrow, T. Sawata, and M. Holme, "A Wide – Speed – Range Hybrid Variable – Reluctance / Permanent – Magnet Generator for Future Embedded Aircraft Generation Systems," IEEE Trans. On Industry Applications, Vol. 41, No. 2, PP. 551 – 556, March/April 2005.

[6] M. Sadeghierad, H. Lesani, H. Monsef, and A. Darabi, "Design considerations of High Speed Axial Flux permanent magnet Generator with Coreless Stator," The 8th International Power Engineering Conference (IPEC), pp. 1098 – 1102, 2007.

[7] D. P. Arnold, S. Das, J. W. Park, I. Zana, J. H. Lang, and M. G. Allen, "Micro fabricated High-Speed Axial-Flux Multi watt Permanent- Magnet Generators—Part II: Design, Fabrication, and Testing," Journal Of Micro Electromechanical Systems, Vol. 5, No. 5, pp. 1351 – 1363, October 2006.

[8] J. J. H. Paulides, G. W. Jewell, and D. Howe, "An Evaluation of Alternative Stator Lamination Materials for a High – Speed, 1.5 MW, Permanent Magnet Generator," IEEE Trans. On Magnetics, Vol. 40, No. 4, pp. 2041 - 2043, July 2004.

[9] S. M. Jang, H. W. Cho, and Y. H. Jeong, "Influence on the rectifiers of rotor losses in high – speed permanent magnet synchronous alternator," Journal of Applied Physics, 08R315, American Institute of Physics, 08R315-1 - 08R315-3, 2006.

[10] Z. Kolondzovski, "Determination of critical thermal operations for High – speed permanent magnet electrical machines," The International Journal for Computation and Mathematics in Electrical and Electronic Engineering, Vol. 27 No. 4, pp. 720-727, 2008.
[11] A. S. Nagorny, N. V. Dravid, R. H. Jansen, and B. H. Kenny, "Design Aspects of a High Speed Permanent Magnet Synchronous Motor / Generator for Flywheel Applications," NASA/TM—2005-213651 June 2005, International Electric Machines and Drives Conference sponsored by the IEEE Industry Applications Society, IEEE Power Electronics Society, IEEE Power Engineering Society, and IEEE Industrial Electronics Society, San Antonio, Texas, May 15–18, 2005.
[12] D. C. Hanselmann, Brushless Permanent Magnet Motor Design, New York: McGraw-Hill, 1994.
[13] J. R. Hendershot and T. J. E. Miller, Design of Brushless Permanent Magnet Motors, Oxford, U.K.: Magna Physics Publishing and Clarendon Press, 1994.
[14] J. E. Rucker, J. L. Kirtley, Jr. T. J. McCoy, "Design and Analysis of a Permanent Magnet Generator For Naval Applications," IEEE Electric Ship Technologies Symposium, pp. 451 – 458, 2005.
[15] D. Kang, P. Curiac, Y. Jung, and S. Jung, "Prospects for magnetization of large PM rotors: conclusions from a development case study," IEEE trans. On Energy Conversion, vol. 18, no. 3, Sept. 2003.
[16] J. Paulides, G. Jewell, and D. Howe, "An evaluation of alternative stator lamination materials for a high speed, 1.5 MW, permanent Magnet Generator," IEEE Trans. On Magnetics, vol. 40, no. 4, July 2004.
[17] N. Bianchi, and A. Lorenzoni, "Permanent magnet generators for wind power industry: an overall comparison with traditional generators," Opportunities and advances in international power generation, conference publication No. 419, 1996.
[18] M. A. Rahman, and G. R. Slemon, "Promising Applications of Neodymium Iron Boron Iron Magnets in Electrical Machines," IEEE Trans. On Magnetics, Vol. No. 5, Sept 1985.
[19] H. Polinder and M. J. Hoeijmakers, "Eddy – Current Losses in the Segmented Surface Mounted Magnets of a PM Machine," IEE Proceedings, Electrical Power Applications, Vol. 146, No. 3, May 1999.
[20] O. Aglen, and A. Andersson, "Thermal Analysis of a High Speed Generator," Industry Applications Conference, 2003. 38th IAS Annual Meeting. Conference, vol.1, pp. 547- 554, 12-16 Oct. 2003. Current Version Published: 2004-01-07 IEEE Transactions, 2003.
[21] J. Pepi, and P. Mongeau, " High power density permanent magnet generators," DRS Electric power technologies, Inc., 2004.
[22] I. Boldea and S. A. Nasar, Induction Machine Handbook, CRC Press, Boca Raton, Fl, 2001.
[23] B. Amin, "Contribution to iron-loss evaluation in electrical machines", European Trans. on Elect. Power Eng., vol. 5, 1995, pp. 325-332.
[24] Z.Q. Zhu, D. Howe, E. Bolte, B. Ackermann, "Instantaneous Magnetic Field distribution in brushless permanent-magnet dc motors, part I: open-circuit field", IEEE Trans. on Magnetics, vol. 29, 1993, pp. 124-135.
[25] Z.Q. Zhu, D. Howe, "Instantaneous Magnetic Field distribution in brushless permanent-magnet dc motors, part II: armature-reaction field", IEEE Trans. on Magnetics, vol. 29, 1993, pp. 136-142.
[26] Z.Q. Zhu, D. Howe, "Instantaneous Magnetic Field distribution in brushless permanent-magnet dc motors, part III: effect of stator slotting", IEEE Trans. on Magnetics, vol. 29, 1993, pp. 143-151.
[27] Z.Q. Zhu, D. Howe, "Instantaneous Magnetic Field distribution in brushless permanent-magnet dc motors, part IV: magnetic field on load", IEEE Trans. on Magnetics, vol. 29, 1993, pp. 152-158.
[28] J.G. Zhu, S.Y.R. Hui, V.S. Ramsden, "Discrete modelling of magnetic cores including hysteresis, eddy current, and anomalous losses", IEE Proc., Part A, Sc., Measure. and Tech., vol. 140, 1993, pp. 317-322.
[29] I. Boldea, Variable speed electric generators, CRC Press, Florida, 2006.
[30] J.G. Zhu, S.Y.R. Hui, V.S. Ramsden, "A generalized dynamic circuit model of magnetic cores for low- and high-frequency applications - Part I: Theoretical calculation of the equivalent core loss resistance", IEEE Trans. Power Elect., vol. 11, 1996, pp.246-250.
[31] X. Kong, F. Wang, and Y. Sun, "Comparison of High Speed PM Generator with PM Doubly Fed Reluctance Generator for Distributed Power Generation System," 2nd IEEE Conference on Industrial Electronics and Applications, 2007. ICIEA 2007, pp. 1193 – 1197, 23-25 May 2007.
[32] Y. Chen, P. Pillay, and A. Khan, "PM wind generator comparison of different topologies," Industry Applications Conference, 2004. 39th IAS Annual Meeting. Conference Record of the 2004 IEEE vol.3, pp. 1405 - 1412, 3-7 Oct. 2004.
[33] Moré, J.J. and D.C. Sorensen, "Computing a Trust Region Step," SIAM Journal on Scientific and Statistical Computing, Vol. 3, pp 553-572, 1983.
[34] Zhang, Y. , "Solving Large-Scale Linear Programs by Interior-Point Methods Under the MATLAB Environment," Department of Mathematics and Statistics, University of Maryland, Baltimore County, Baltimore, MD, Technical Report TR96-01, July, 1995.

[35] Conn, A. R., N. I. M. Gould, and Ph. L. Toint, "A Globally Convergent Augmented Lagrangian Algorithm for Optimization with General Constraints and Simple Bounds," SIAM Journal on Numerical Analysis, Volume 28, Number 2, pages 545–572, 1991.

[36] Conn, A. R., N. I. M. Gould, and Ph. L. Toint, "A Globally Convergent Augmented Lagrangian Barrier Algorithm for Optimization with General Inequality Constraints and Simple Bounds," Mathematics of Computation, Volume 66, Number 217, pages 261–288, 1997.

Biographical notes:

Adel El Shahat is currently a Research Scientist, ECE Dept., Mechatronics-Green Energy Lab, The Ohio State University, USA. His interests are: Electric Machines, Artificial Intelligence, Renewable Energy, Power System, Control Systems, PV cells, Power Electronics, and Smart Grids. He has nearly 60 publications between international Journals papers, refereed conferences papers, book chapters and abstracts or posters. He is a Member of IEEE, IEEE Computer Society, ASEE, IAENG, IACSIT, EES, WASET and ARISE. Also, he is member of editorial team and reviewer for six international journals. He gains honors and recognitions from OSU, USA 2009, Suez Canal University Honor with university Medal in 2006, Merit Ten Top-up Students Award of each Faculty from Arab Republic of Egypt, in 2000, and EES, 1999, Egypt.

Ali Keyhani was with the Hewlett-Packard Company and TRW Control from 1967 to 1972. Currently, he is a Professor of Electrical Engineering at The Ohio State University (OSU), Columbus. He serves as the Director of the OSU Electromechanical and Mechatronic Systems Laboratory. His research activities focus on the control of smart grid systems, distributed energy systems, the design and modeling of electric machines, the control and design of power electronic systems, the DSP-based virtual test bed for design, and the control of power systems, automotive systems, modeling, parameter estimation, and failure detection systems. Dr. Keyhani received the OSU College of Engineering Research Award in 1989, 1999, and 2003. He was an Editor for the IEEE Transactions on Energy Conversion and past Chairman of the Electric Machinery Committee, IEEE Power Engineering Society.

Hamed El Shewy currently is a Professor of Electrical Machines in the Electrical Power and Machines Department, Faculty of Engineering, Zagazig University, Zagazig, Egypt. He was the previous head of the same department. His research interests include Electric Machines, Power Systems, Power Electronics, and Electric Drives.